

# Wave Energy Resource Analysis for Use in Wave Energy Conversion

**Jeremiah Pastor**

Department of Mechanical Engineering,  
University of Louisiana at Lafayette,  
Lafayette, LA 70504  
e-mail: jeremiah@louisiana.edu

**Yucheng Liu**

Department of Mechanical Engineering,  
Mississippi State University,  
Mississippi State, MS 39760  
e-mail: liu@me.msstate.edu

*In order to correctly predict and evaluate the response of wave energy converters (WECs), an accurate representation of wave climate resource is crucial. This paper gives an overview of wave resource modeling techniques and applies a methodology to estimate the naturally available and technically recoverable resource in a given deployment site. The methodology was initially developed by the Electric Power Research Institute (EPRI), which uses a modified Gamma spectrum to interpret sea state hindcast parameter data produced by National Oceanic and Atmospheric Administrations (NOAA's) Wave-watch III. This Gamma spectrum is dependent on the calibration of two variables relating to the spectral width parameter and spectral peakedness parameter. In this study, this methodology was revised by the authors to increase its accuracy in formulating wave length. The revised methodology shows how to assess a given geographic area's wave resource based on its wave power density and total annual wave energy flux.*

[DOI: 10.1115/1.4028880]

*Keywords: wave spectra, wave climate analysis, wave power absorption, wave power density, wave energy flux*

## 1 Introduction

In order to give an adequate forecast of the long-term energy output of a WEC, it becomes necessary to find the response in full range of sea states at a given deployment site where the WEC is deployed. Because of the time factor, it is impractical to calculate this response for every measured wave spectra at that site when simulating a WEC or an array of WECs. In lieu of this, a systematic method is needed to parameterize the wave resource for a given site so that a WEC's response can be calculated for a finite range of values for significant wave height ( $H_s$ ) and the peak wave period ( $T_p$ ), from which its performance in other sea states can be easily estimated through numerical interpolation. At present, WEC developers utilize an approach that represents a WEC's power production by means of a power matrix in terms of  $H_s$  and  $T_p$ . This is proved to be inadequate due to the fact that there can be a wide range of spectral shapes for a given  $H_s$  and  $T_p$ , which can result in a large variation in the power produced relative to the value listed in the power matrix [1].

In the past, there have been a number of approaches that had been used to address the limited descriptive ability of the power matrix. Preliminary wave energy device performance protocol presented by the Department of Trade and Industry (DTI) in UK implies that several tables outlining the mean, standard deviation, minimum and maximum power for each cell of the power matrix can be used to describe the response of a WEC [2]. This technique is relatively simple to use, however, the distribution of spectral shapes for a given  $H_s$  and  $T_p$  is likely to vary with the location so that a set of tables would need to be generated for each site of interest, which can be very laborious and time consuming.

In an effort to overcome this deficiency, an approach was developed which include more parameters to describe the power response. Several studies were conducted to examine the sensitivity of power output to a variety of spectral bandwidth parameters by using the developed approach [3,4]. In those studies, it was

suggested that 3D power matrices should be used to describe a waver conversion device's power response, partitioned by  $H_s$ ,  $T_p$ , and spectral bandwidth. The obtained results showed that while the use of certain bandwidth parameters can improve the accuracy of predicted performance of certain WECs at certain locations over a range of conditions, there was no single bandwidth parameter which was effective at predicting performance of all types of WEC at any locations and under any conditions.

Kerbirou et al. [5,6] proposed a slightly different approach in which the measured spectra are partitioned into separate wave systems, each of which is represented by a modified JONSWAP spectrum. The power response is then calculated as the sum of the contributions from each component wave system. This method was proven to significantly improve the accuracy of the energy yield assessment, but at the expense of introducing more parameters (overall six parameters are used) in describing the directional characteristics of the spectrum. The disadvantage of using more parameters in the approach is that a large number of points are required to cover the parameter space in order to describe the full range of sea states at a given deployment site.

Duclos et al. [7] showed that optimizing the WEC necessitates accounting for all possible wave conditions weighted by their annual occurrence frequency, as generally given by the classical wave climate scatter diagrams. A generic and simple WEC was also presented to show how the optimal parameters depend on the very different wave climate. Besides that, the influence of the wave climate on the design and annual production of electricity by OWC wave power plants was also investigated by Sarmento et al. [8].

Based on the current progress made in wave resource description and WEC power response evaluation, this paper will continue to review different models for omnidirectional wave spectra and then outline and revise a systematic methodology to estimate two quantities for characterizing the naturally available wave energy resource in a given area as given by the EPRI [9]. The EPRI method is based on a calibration of spectral width parameter,  $n$ , which is observed to have a significant influence on the wave power density and is proved to be robust in all ocean regions evaluated including the North Pacific Ocean, Gulf of Mexico, and the

Contributed by the Ocean, Offshore, and Arctic Engineering Division of ASME for publication in the JOURNAL OF OFFSHORE MECHANICS AND ARCTIC ENGINEERING. Manuscript received November 26, 2013; final manuscript received October 16, 2014; published online November 17, 2014. Assoc. Editor: Krish Thiagarajan.

Caribbean Sea. Remaining sections of this paper are organized as follows: Section 2 describes the standard spectral models; Sec. 3 presents a five-step technical approach for estimating the wave energy resource, the wave power density values, and the annual wave energy flux in a given region; Sec. 4 presents a case study to apply this method to estimate the available wave energy for a localized geographic location and validate the results by comparing to current data; and the entire paper is concluded in Sec. 5.

## 2 Omnidirectional Wave Spectral Models

Equation (1) [10] gives a family of equations which are most commonly used for assessing the unimodal spectra

$$S(f) = \alpha f^{-r} \exp(-\beta f^{-s}) \gamma^{\alpha(f)} \quad (1)$$

Here  $\alpha, \beta, r, s > 0$ , and  $\gamma \geq 1$ , and

$$a(f) = \exp\left(-\frac{1}{2} \left(\frac{f - f_p}{\sigma f_p}\right)^2\right) \quad (2)$$

$$\sigma = \begin{cases} 0.07 & \text{for } f < f_p \\ 0.09 & \text{for } f \geq f_p \end{cases} \quad (3)$$

The parameters  $r$  and  $s$  control the shape of the spectrum,  $\alpha$  is the scale parameter,  $\beta$  is the location parameter (in terms of frequency), and  $\gamma$  is known as the peak enhancement factor. The peak frequency of the spectrum is given by

$$f_p = (s\beta/r)^{1/s} \quad (4)$$

The family of spectra defined in Eq. (1) has five free parameters. In order to describe the sea state with fewer variables, Eq. (1) was converted to different forms by fixing some parameters with constant values while leaving the others free. For example, let  $r = 5$ ,  $s = 4$ , and  $\gamma = 1$ , Eq. (1) then becomes the popular Bretschneider form Ref. [11]. A special form of the Bretschneider spectrum for fully developed seas was proposed by Pierson and Moskowitz [12], where  $\alpha$  is fixed and the energy in the spectrum depends on the value of  $\beta$  only, the ratio  $H_s/T_p$  is fixed as well. The JONSWAP form Ref. [13] is a further generalization of Bretschneider spectra, which accounts for the more peaked spectral shapes observed in the fetch-limited wind seas. Ochi and Hubble [14] advocated the use of such form where  $s = 4$ ,  $\gamma = 1$ , and  $r$  is a free parameter. Finally, Boukhanovsky et al. [15,16] presented a "Gamma spectra" form where  $\gamma = 1$  and  $s = (r - 1)$ , which serves as the basis of the methodology used in our study.

Figure 1 shows examples of the JONSWAP, Ochi, and Gamma families for fixed  $H_s$  and  $f_p$  and a range of  $\gamma$  (the other two are  $\alpha$  and  $\beta$ ). In each plot the Bretschneider spectrum is a special case and is indicated with a bold line. For the JONSWAP family the Bretschneider spectrum is the limiting form, corresponding to the most broad-banded member. As the peak enhancement factor increases, the spectrum becomes more peaked, but a spread of energy remains between about  $0.6f_p$  and  $2f_p$ . Gamma and Ochi spectra can take more broad-banded forms than the JONSWAP spectra, albeit with the possibility of a physically unrealistic amount of energy in the tail for low values of  $r$ . For Ochi spectra there is little variation in the shape for frequencies less than  $f_p$ , whereas for the Gamma spectra the proportion of energy below  $f_p$  increases as  $r$  decreases. For higher values of  $r$ , both the Gamma and Ochi spectra can have an arbitrarily narrow concentration of energy about the peak frequency  $f_p$ .

For spectra with three parameters,  $\gamma$  controls the bandwidth or equivalently the peakedness of the spectrum. Here the peakedness of a spectrum is defined as the ratio  $S(f_p)/S_{p0}$ , where  $S_{p0}$  is the peak spectral density of a Bretschneider spectrum with the same  $H_s$  and  $T_p$ , given by

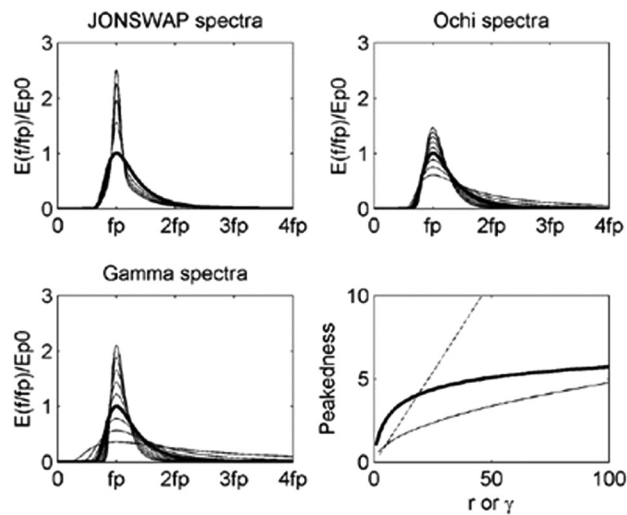


Fig. 1 Normalized shapes of JONSWAP spectra for  $\gamma = 1-5$  and Ochi and Gamma spectra for  $r = 2-10$ . In each plot the Bretschneider spectrum is shown in bold. The peakedness of each type of spectrum is shown in the lower right plot as a function of  $\gamma$  for the JONSWAP spectrum (bold line) and  $r$  for the Ochi spectra (thin line) and Gamma spectra (dashed line).

$$S_{p0} = H_s^2 T_p \frac{\exp(-5/4)}{4\Gamma(5/4)} \left(\frac{5}{4}\right)^{5/4} \quad (5)$$

The peakedness of the JONSWAP, Ochi, and Gamma spectra are shown in Fig. 1. From that figure it can be seen that the peakedness increases approximately linearly with respect to  $r$  for the Gamma spectra, and approximately logarithmically with respect to  $r$  and  $\gamma$  for Ochi and JONSWAP spectra, respectively. In fact, the peakedness of the JONSWAP spectrum can be empirically approximated as  $1 + \ln(\gamma)$  for  $\gamma < 100$ .

The most commonly used multimodal spectral shapes are formulated as the summation of either JONSWAP, Gamma, or Ochi spectra. For example, Boukhanovsky et al. [15,16] used multimodal spectra as the sum of Gamma spectra in their study. Ochi and Hubble [14] proposed a six-parameter spectrum formed as the sum of two Ochi spectra. Soares [17] proposed a bimodal spectrum formed as the sum of two JONSWAP spectra, but with  $\gamma$  fixed as two for both components, resulting in a four-parameter spectrum. There are also other forms composed as the sum of two JONSWAP spectra, as proposed by Torsethaugen [18,19].

In this paper, the use of the Gamma spectra will be modified to include two spectral shape coefficients. The calibration objective is to find values of these coefficients for a given region through an iterative process in order to reconstruct the overall sea state spectra that would be best fit the full hindcast spectra for that given region of a selected deepwater calibration station.

## 3 Methodology for Estimating the Available Wave Energy Resource

In a recent study conducted by the EPRI, data was collected from U.S. coastal waters for a 51-month Wavewatch III hindcast database that was developed specifically for the EPRI by the National Center for Environmental Prediction (NCEP) of NOAA [20]. The EPRI's method was validated by comparing the Wavewatch III hindcast results with the wave measurements recorded during the same time period. According to this methodology, two quantities will be found and estimated for characterizing the naturally available wave energy resource in a given site. Those two quantities are the wave power density (KW per meter of wave crest width) and the total annual wave energy flux (TW-h per

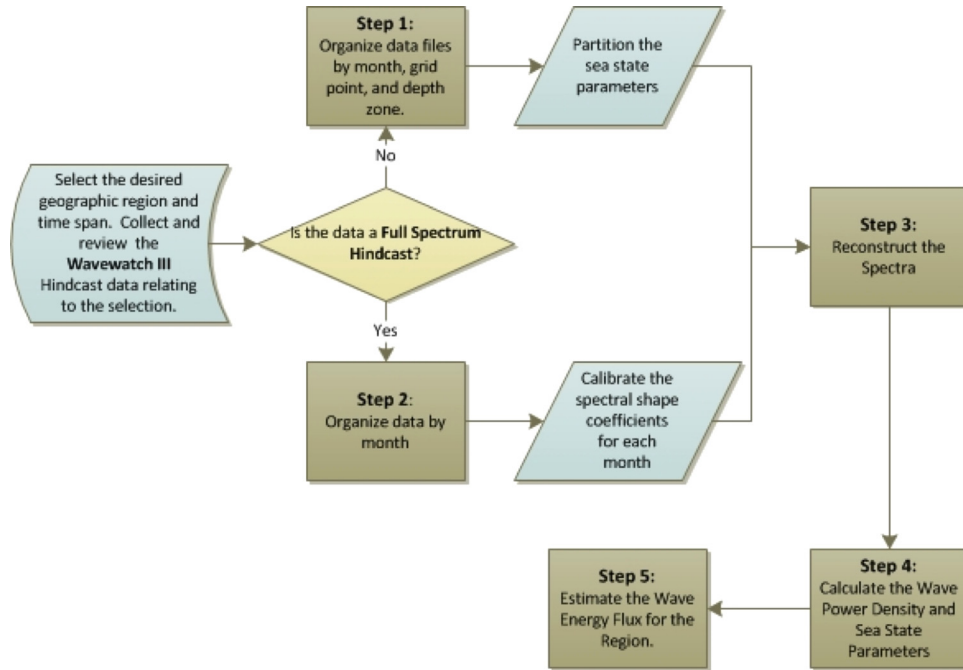


Fig. 2 A flowchart of finding the wave power density and annual wave energy flux

year). Five major steps need to be followed to obtain these two quantities. A flowchart showing this five-step method is plotted in Fig. 2.

**3.1 Preprocess Wavewatch III Multipartition Hindcast of Sea State Parameters.** In step one, the large gridded hindcast data files produced by NCEP are preprocessed and converted into a more usable and accessible database structure. Wavewatch III solves the random phase spectral action density balance equation for wavenumber-direction spectra. In this equation it is assumed that properties of medium (water depth and current) as well as the wave field itself vary on time and space scales that are much larger than the variation scales of a single wave. The raw data (grid points) given from the Wavewatch database are the full directional spectrum data (in frequency domain), which need to be first converted to the nondirectional data (in time domain) and organized into its time slot. The conversions will be performed by the Wavewatch III model at 3h intervals for all grid points. Due to the fact that the full directional spectrum contains such a vast amount of information (24 directions  $\times$  25 frequency bins = 600 values per hindcast), the full directional spectrum is only achieved for 275 grid points around the world. If a full directional spectrum is available then these values need to be converted into the nondirectional wave spectrum.

**3.1.1 Calculating Nondirectional Spectrum From Directional Spectrum.** The term “nondirectional spectrum” here is referred as the “nondirectional wind wave sea surface elevation variance density spectrum,” which is the integral of the directional wave spectrum over all directions ( $d\theta$ ) at each frequency. Therefore, given  $S(f, \theta)$  as the directional wave spectrum in  $m^2/Hz$  rad, then the nondirectional wave spectrum  $S(f)$  is in  $m^2/Hz$  and can be calculated as follows:

$$S(f) = \int_0^{2\pi} S(f, \theta) d\theta = \Delta\theta \sum_{i=1}^N S(f, \theta_i) = \frac{2\pi}{N} \sum_{i=1}^N S(f, \theta_i) \quad (6)$$

where  $N$  is the number of bins, which is 24 in Wavewatch III model;  $\theta$  is the wave direction in radians; and  $f$  is the frequency in

Hz. Now that the nondirectional wave spectrum is established, the spectral moments needed for calibration can be found.

**3.1.2 Calculating the Spectral Moments From the Nondirectional Spectrum.** In order to calibrate the spectral shape coefficients and calculate the sea state parameters from the nondirectional wave spectrum, the  $n$ th spectral moment needs to be defined as

$$m_n = \int_0^{\infty} f^n S(f) df = \sum_{i=1}^N (f_i)^N S(f_i) \Delta f \quad (7)$$

where  $N$  is the number of frequency bins, which is 25 for the Wavewatch III database and  $\Delta f_i$  is the frequency bin width for the  $i$ th bin.

In order to establish an iterative process, two initial spectral moments  $m_0$  and  $m_{-1}$  are defined as

$$m_0 = \sum_{i=1}^N S(f_i) \Delta f_i \quad (8)$$

$$m_{-1} = \sum_{i=1}^N \frac{S(f_i)}{f_i} \Delta f_i \quad (9)$$

These moments are required for calculating the significant wave height, wave energy period, and wave power density.

The remaining grid points only include three sea state parameters: spectrally derived significant wave height ( $H_{m0}$ ), peak wave period ( $T_p$ ), and mean direction of spectral peak energy ( $\theta_p$ ). Though such a database of fully partitioned sea state parameters does not provide as much information as contained in the full directional spectrum, the information is sufficient enough to reconstruct the nondirectional spectrum by applying a theoretical spectral formulation to each partition, and then summing the remaining spectra across all partitions or component wave trains. This will be completed in step 2. Before that, the large gridded hindcast data files produced by the NCEP need to be preprocessed into a more usable and accessible database structure.

```

WAVEWATCH III PARTITIONED DATA FILE III 1.01
yyyyymmdd hhhmss lat lon name nprt depth uabs udir cabs cdir
0 hs0 tp0 lp0 theta0 sp0 wf0
1 hs1 tp1 lp1 theta1 sp1 wf1
.
.
.
N hsN tpN lpN thetaN spN wfN

```

where:

```

yyyyymmdd Date in 4-digit year, 3-digit month, 3-digit day format
hhhmss Time in 3-digit hour, 3-digit minute, 3-digit second format
lat Latitude in decimal degrees
long Longitude in decimal degrees; for Western Hemisphere values,
subtract 360 to yield form of -xxx.xx, where negative sign
indicates longitude is xxx.xx degrees west of Prime Meridian
name 'grid_point' for all grid points
nprt, N Number of component wave train partitions in overall sea state
depth Water depth in meters
uabs Wind speed at 10 meters above sea level, in meters per second
udir Direction from which wind is blowing, in degrees
cspd Surface current speed, in meters per second
cdir Direction towards which current is flowing, in degrees

```

**For each partition at given grid point, the following parameters are listed:**

```

hs Significant wave height of partition spectrum, in meters,
calculated by NOAA as four times the square root of the
zeroeth spectral moment (Equation 4 of Appendix A). In
its hindcast data files, NCEP uses the abbreviation "hs"
rather than the "Hm0" term adopted in this report.
tp Peak wave period, in seconds, corresponding to center of
frequency bin at which partition spectrum has maximum energy
lp Wavelength corresponding to peak wave period, in meters
theta Spectrally weighted mean direction towards which wave energy in
frequency bin of peak spectral energy is traveling
sp Total directional spread of partition spectrum, in degrees
wf Fraction of partition spectrum that is forced by local wind

```

**Note that '0' in the first line of the partition listing refers to the overall sea state (all partitions combined)**

Fig. 3 NCEP file structure for Wavewatch III Hindcast data [20]

3.1.3 *Organizing the Directional Data.* After having the nondirectional data, those data have to be sorted and organized into a database structure. In order to do that, the grid points for specific geographic area and mapping limitations will be selected and the selected points will then be organized into a file structure that has all the time steps for a given month as an individual file for each grid point.

The way that the Wavewatch III hindcast file produced by NCEP is structured by month such that the multipartition sea state parameter data are given for every grid point throughout a given geographic domain of the file at a particular time step, and then the entire grid repeats for the next time step (after an interval of 3 h). Typically the large gridded domains have a spacing of 4 min in longitude and latitude. In preprocessing the data, only the grid points for your specific geographic area and mapping limitations

will be selected and organized into a file structure that has all the time steps for given months as an individual file for each grid point. Figure 3 presents an example of the organized data structure, which shows a sorting of files by region, depth zone, grid point, and month.

3.2 **Calibrate the Spectral Shape Coefficients.** From the sea state parameters given, the wave power density needs to be accurately calculated. In the present methodology, a modified Gamma spectrum will be reconstructed and applied to each sea state partition. This modified Gamma spectrum has two spectral shape coefficients. In order to find these coefficients a calibration process needs to be performed to find their values for a given region so as to reconstruct the overall sea state spectra that would be best fit

the full hindcast spectra for that region from a selected deepwater calibration station.

It can be observed that the wave power density is directly proportional to  $m_{-1}$  of the wave spectrum (Eq. (28)). The calibration technique developed by EPRI attempts to minimize the difference between the reconstructed spectrum and the full spectrum for  $S(f)/f$ , which is the integrand of  $m_{-1}$  (Eq. (9)). The root-mean-square (RMS) difference in  $S(f)/f$  between the reconstructed spectrum and the full hindcast spectrum over the entire range of frequencies for a particular time step will be first calculated. The RMS differences will then be aggregated over all time steps in a given month–year combination. Next, the shape coefficient ( $k_b$ ) value that leads to the least aggregate RMS difference can be found. Subsection 3.2.1 explains the formula for finding the wave spectrum, Sec. 3.2.2 introduces how to calibrate the coefficients variable  $n$ , and  $\gamma$  that are used for the formula presented in Sec. 3.2.1. The procedure for minimizing the RMS to get  $k_b$  is basically the process of calibrating the coefficient  $n$ , which will be demonstrated in Sec. 3.2.2. This procedure is demonstrated through following equations.

**3.2.1 Theoretical Gamma Spectral Formulation.** The spectral formulation for a single wave train or partition developed by EPRI is derived from the basic Gamma ( $\Gamma$ ) spectrum equation as

$$S_{\Gamma}(f) = \frac{A}{f^n} \exp\left[-\frac{B}{f^{(n-1)}}\right] \gamma^a \quad (10)$$

where

$$A = n \frac{H_{m0}^2}{T_p^4} \quad (11)$$

$$B = \frac{n}{T_p^4} \quad (12)$$

In these equations,  $n$  is the spectral width parameter and  $\gamma$  is the spectral peakedness parameter. The exponent parameter,  $a$ , defines the asymmetry around the spectral peak and is a function of  $f$  according to the following formula:

$$a = \exp\left[-\frac{(f - f_p)^2}{\sigma^2 f_p^2}\right] \quad (13)$$

where  $\sigma$  is defined in Eq. (3).

The Gamma spectrum becomes the Bretschneider spectrum when  $n = 5$  and  $\gamma = 1$ , whose shape depends only on two sea state parameters  $H_{m0}$  and  $T_p$ . The Gamma spectrum becomes the JONSWAP spectrum when  $n = 5$  and  $\gamma > 1$ , which has a peak overshoot characteristic for developing seas. Following Ochi and Hubble approach [14], a full spectrum can be reconstructed at the sum of Gamma spectra by calibrating either  $n$  or  $\gamma$ .

### 3.2.2 Calibrating $n$ and $\gamma$ for Use in the Gamma Spectra.

Within any given hindcast partition, there are two types of wave trains that can be represented by the shape factors  $n$  and  $\gamma$ . The type I sea state refers to the developing wind seas so we set  $n = 5$  and calibrate  $\gamma$  using Eq. (13) to define the spectral peak asymmetry. The type II sea state refers to all other sea states (swells, decaying wind seas, and fully developed wind seas), for such type we set  $\gamma = 1$  and calibrate the spectral width parameter,  $n$ .

The type I sea state is defined for the developing wind seas and in order for such seas to grow the spectrum, the actual wave period needs to be longer than the peak period  $T_p$ . This is due to the fact the waves that characterize shorter periods have already reached the steepness required for equilibrium and cannot grow higher without destabilizing or breaking. Within the spectra there exists a long-period cutoff, above which the wave energy in the

spectra is traveling faster than the wind. This is because the wave group velocity is directly proportional to wave period. As long as the spectral peak period is less than the long-period cutoff, the spectrum can still develop further.

Another advantage of the Wavewatch III hindcast data is that it also produces local wind speed along with the sea state parameters. This advantage allows us to estimate the long-period cutoff using the Pierson–Moskowitz relationship [12]. Such relationship can be used to identify the developing seas in the hindcast partitions. The Pierson–Moskowitz theoretical peak period for a fully developed sea state in complete equilibrium with the local wind speed, however, can be used as the long-period cutoff. There is an inconsistency due to the fact that the Pierson–Moskowitz relationship is given at an elevation of 19.5 m above sea level and the Wavewatch III hindcast wind speed data is given at 10 m above sea level. In order to apply the Pierson–Moskowitz relationship for the Wavewatch III hindcast data, a 1/7-power law for the shear profile in the marine boundary is employed [20–22]. The peak wave period for fully developed seas  $T_{pFD}$  can be calculated as

$$T_{pFD} = \frac{2\pi U_{10} (1.95)^{(1/7)}}{0.87g} = \frac{7.9450 U_{10}}{g} = 0.81016 U_{10} \quad (14)$$

where  $U_{10}$  is the Wavewatch III hindcast wind speed at 10 m above sea level and  $g$  is the gravitational acceleration, which is 9.81 m/s<sup>2</sup>.

Once  $T_{pFD}$  is found then it can be compared to the Wavewatch III hindcast peak period ( $T_p$ ) for that given partition. If  $T_p < T_{pFD}$ , then that partition is considered to be in a developing wind sea state and can be labeled as a type I sea state and calibrated accordingly as stated above. If  $T_p > T_{pFD}$ , then the partition is labeled as a type II sea state and  $n$  needs to be determined as

$$n = 5wf + k_b T_p (1 - wf) \quad (15)$$

In Eq. (15),  $T_p$  is the Wavewatch III hindcast peak period of the partition and  $wf$  is the hindcast wind fraction of the partition, which refers to the fraction of energy in a given partition forced by local winds. Note that the calibrated value of  $k_b$ , as discussed above is now implemented as a dimensional constant which models the dependency of the spectral width on the peak.

From Eq. (15), if  $wf = 1$ , then  $n$  is calculated as five, the spectrum becomes the Bretschneider spectrum, which is appropriate for seas under the influence of local winds with no swell energy present. It was found by EPRI that  $k_b$  indicates the spectral width of wave energy that is not influenced by the local winds [9]. It is the value of  $k_b$  that is calibrated which in turn determines  $n$  from Eq. (15) (as shown in Fig. 4).

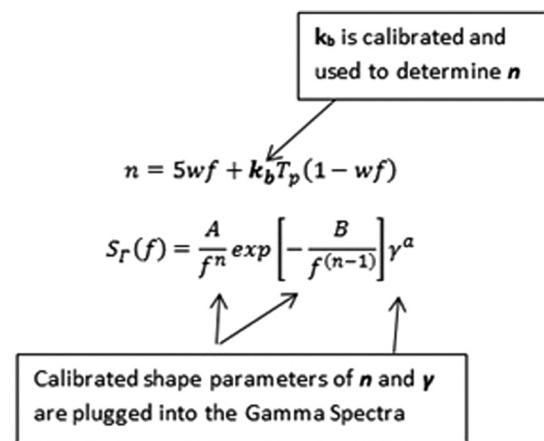


Fig. 4 Calibrated parameters for the Gamma spectra

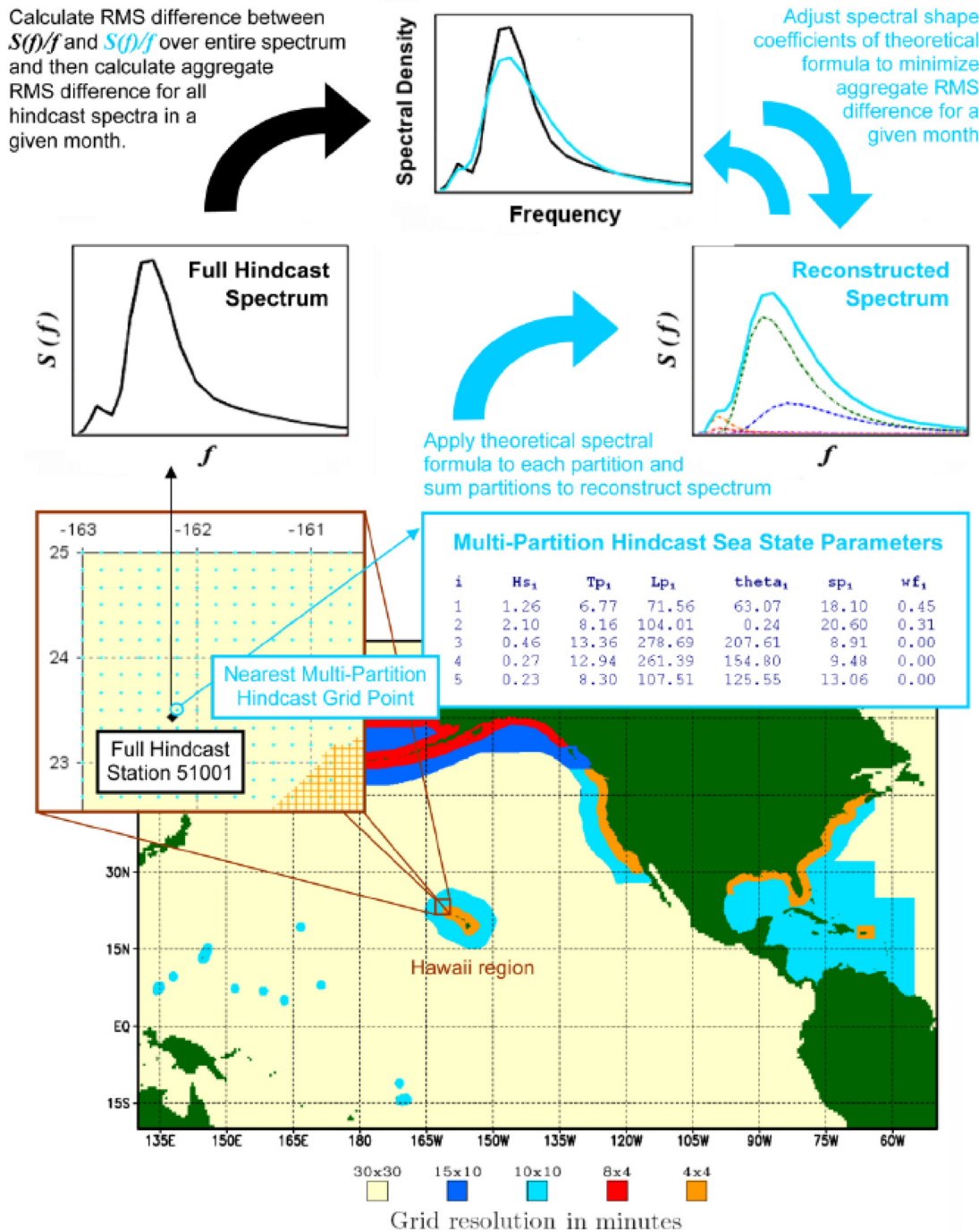


Fig. 5 Process for calibrating theoretical spectra reconstructed from sea state parameters

**3.3 Reconstruct the Overall Spectra.** In this step, the overall spectra can be reconstructed using the spectral shape parameters calibrated in previous steps, as Eq. (10). By using the two data inputs (the hindcast sea state parameter data and the spectral shape coefficient data) for each partition in the given region, the spectra and the quantities listed in step 4 can be calculated for each time step in a given month. If the time period of interest is 12 months, then there would be approximately 2920 hindcast time steps (the time interval is 3h) on each grid point. The overall number of reconstructed overall sea state spectra during a 12-month period will then be equal to 2920 times the number of grid points in the region of interest. This reconstruction process is depicted in Fig. 5.

**3.4 Calculate Overall Sea State Parameters and Wave Power Density.** In order to reconstruct the overall sea state spectrum, three parameters have to be decided, which consist of the significant wave height, the wave energy period, and the wave power density.

The first value is the spectrally derived significant wave height ( $H_{m0}$ ), which can be calculated as

$$H_{m0} = 4\sqrt{m_0} \quad (16)$$

This value approximates time-series derived significant wave height, which is the average of the highest third of the waves in a

random seaway and generally corresponds to the mean wave height that could be estimated by visual observation due to the fact that the smaller waves can pass undetected by the human eyes. This figure was calculated and archived by Wavewatch III and can be found from Ref. [20].

The wave energy period ( $T_e$ ) can be determined from the two spectral moments ( $m_{-1}$  and  $m_0$ ) calculated above, as

$$T_e = \frac{m_{-1}}{m_0} \quad (17)$$

The wave energy period is a sea state parameter that is not needed for further calculations, therefore is not archived in Wavewatch III.

The energy period  $T_e$  is rarely specified and must be estimated from other variables when the spectral shape is unknown. For example, in preparing the Atlas of UK marine renewable energy resources, it was assumed that  $T_e = 1.14T_z$  [23]. Alternatively, it can be estimated based on  $T_p$  as

$$T_e = \alpha T_p \quad (18)$$

The coefficient  $\alpha$  depends on the shape of the wave spectrum:  $\alpha = 0.86$  for a Pierson–Moskowitz spectrum, and  $\alpha$  increases toward unity with decreasing spectral width. In assessing the wave energy resource in Southern New England, Hageman [24] assumed that  $T_e = T_p$ . In this study, we adopted the more conservative assumption of  $\alpha = 0.90$  or  $T_e = 0.9T_p$ , which is equivalent to assuming a standard JONSWAP spectrum with a peak enhancement factor of  $\gamma = 3.3$ . It is readily acknowledged that this necessary assumption introduces some uncertainty into the resulting wave power estimates, particularly when the real sea state is comprised of multiple wave systems. However since the wave power density,  $P$ , is proportional to  $T_e H_s$ , errors in period are less significant than errors in wave height.

The peak wave period  $T_p$  is the inverse of the frequency at which the wave spectrum has its highest energy density, and is also referred to as the dominant wave period. This parameter is necessary for formulating the theoretical spectrum and is archived by Wavewatch III.

The mean direction of spectral peak energy ( $\theta_p$ ) is the spectrally weighted mean direction of the wave energy contained within the frequency bin that contains the peak wave period  $T_p$ . This direction is in degrees and measured clockwise from true North, with North staying at 0 deg and East 90 deg. Such parameter is also archived by Wavewatch III.

The total potential and kinetic energy content ( $E$ ) of a wave per unit area of water surface ( $J/m^2$ ) in an irregular sea state can be found as

$$E = \rho g \int_0^\infty S(f) df = \rho g m_0 = \rho g \frac{H_{m0}^2}{16} \quad (19)$$

For each harmonic component of the wave spectrum, its energy travels at the group velocity ( $c_G$ ) as

$$c_G(f, d) = \frac{1}{2} \sqrt{\frac{g}{k} \tan h(kd)} \left( 1 + \frac{2kd}{\sinh(2kd)} \right) \quad (20)$$

where  $g$  is the acceleration due to gravity and  $k$  is the wave number which is given by the dispersion relation

$$(2\pi f)^2 = \left( \frac{2\pi}{T} \right)^2 = gk \tan h(kd) \quad (21)$$

where  $k = (2\pi)/L$ ,  $d$  is the water depth and  $L$  is the wavelength. In deep water, where the local depth is greater than half a wavelength,  $\tan h(kd) \approx 1$  and the dispersion relation can be simplified as

$$\left( \frac{2\pi}{T} \right)^2 = gk \quad (22)$$

so that

$$L_0 = \frac{gT^2}{2\pi} \quad (23)$$

where the subscript “0” denotes deepwater. Therefore the deepwater group velocity can be approximated as

$$c_{G0} = \frac{c}{2} = \frac{L}{2T} = \frac{gT}{4\pi} \quad (24)$$

In an effort to increase the accuracy of the current EPRI method a formulation was found through the U.S. Army Corps of Engineer’s Coastal Engineering Technical Note entitled “Direct methods for calculating wavelength.” In our revised methodology, Eqs. (22) and (23) are replaced by Eqs. (24)–(26), which were proved to be more accurate. Equations (24)–(26) can be derived using Hunt’s method based on the Pade’s approximation, which are accurate to 0.1% for determining the wavelength in any depth of water [25]. It is noticed that there is no subscript “0” in Eq. (24), this is because that that equation can be used for both deep and shallow water

$$L = T \sqrt{\frac{gd}{F}} \quad (25)$$

$$F = G + \frac{1}{1 + 0.6522G + 0.4622G^2 + 0.0864G^4 + 0.0675G^5} \quad (26)$$

$$G = \left( \frac{2\pi}{T} \right)^2 \frac{d}{g} \quad (27)$$

where  $F$  and  $G$  are known as the Pade’s approximation [26].

The wave power density ( $P$ ), which is also referred to as the “wave energy flux,” is given in W/m of wave crest width at any given water depth, and is calculated as

$$P = \rho g \int_0^\infty c_G(f, d) \times S(f) df = \frac{\rho g^2}{4\pi} \int_0^\infty \frac{S(f)}{f} \left[ \left( 1 + \frac{2k_f d}{\sin h(2k_f d)} \right) \tan h(k_f d) \right] df \quad (28)$$

In deep water, the term  $[1 + (2k_f d / \sin h(2k_f d))] \tan h(k_f d) \rightarrow 1$ , therefore above equation is simplified to

$$P_0 = \frac{\rho g^2}{4\pi} m_{-1} = \frac{\rho g^2}{64\pi} T_e (H_{m0})^2 = 490 T_e (H_{m0})^2 \quad (29)$$

From above equation, it is apparently that the wave power density is directly proportional to  $m_{-1}$  of the wave spectrum. In Eq. (28), the seawater density  $\rho$  is 1025 kg/m<sup>3</sup>. Equation (27) shows that the calculation of wave power density always involves the integration of  $S(f)/f$  multiplied by a depth ( $d$ ) and frequency ( $f$ ) dependent dispersion system. Thus, the overall spectrum has to be reconstructed before the wave power density can be determined.

**3.5 Estimating the Total Wave Energy Along a Depth Contour.** In the last step, the total annual wave energy flux (TW-h/yr) will be estimated based on the calculated wave power density for a given area. If the given region involves more than one depth contour, such as a region that incorporates deep water to its nearest shoreline, then the estimation can be a range that reflects the extent to which the deepwater waves traveling toward

**Wave Power Comparison for NOAA Buoy Station #42040**

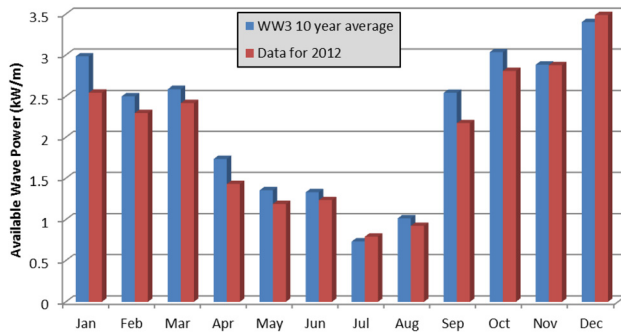


**Fig. 6 Monthly variation in wave power for NOAA buoy station #42040**

the shoreline begin to be significantly affected by the decreasing depth.

#### 4 Calculated Results for a Localized Geographic Location

The method presented in this study was then used to estimate the available wave energy for the NOAA National Data Buoy Center's Station 42040 (LLNR 293)—Luke Offshore Test Platform, which is located about 64 nautical miles south of Dauphin Island, AL [27]. Once the data was analyzed following the steps described in Sec. 3, it was found that the 10 year means for the significant wave height and peak wave period were  $H_s = 1.1$  m and  $T_p = 5.7$  s. A wave energy spectrum was then formulated based on these values (using Eq. (10)), which will be used to assess that area for use with wave energy conversion technology.

In order to validate the wave energy predictions obtained from the presented approach, the calculated results were compared with current data from the NOAA National Data Buoy Center's Station 42040—Luke offshore test platform which is located about 64 nautical miles south of Dauphin Island, AL at  $29^\circ 12' 45''$ N,  $88^\circ 12' 27''$ W. The data is archived and disseminated by the National Data Buoy Center [27].

Based on the data, the monthly variation in the year 2012 for the available wave power (Eqs. (27) and (28)) is plotted in Fig. 6 and compared with the monthly available wave power predictions derived from the 10 year average formulated using the approach presented in Sec. 3 and plotted in Fig. 7. From that figure it can be seen that both the annual mean power and the monthly power variation are in reasonably good agreement. Such agreement can also

**10 Year Average of the Wave Amplitude Spectrum for NOAA Buoy Station 42040**

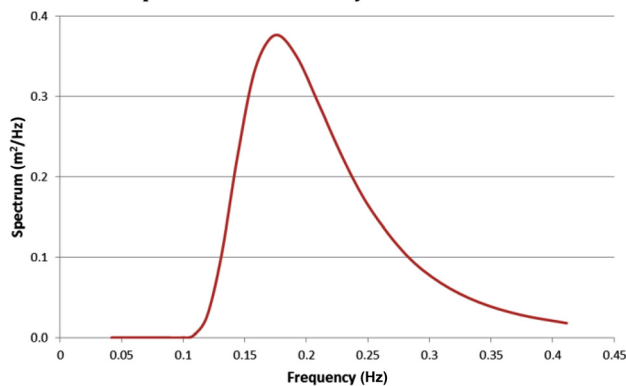


**Fig. 7 10-yr means of the wave energy for NOAA's buoy station #42040 with  $H_s = 1.1$  m and  $T_p = 5.7$  s**

**Table 1 Percent error of the predicted available wave power with respect to the actual available wave power in 2012**

	Predicted power	Current data	% error (%)	EPRI data	% error (%)
Jan.	2983.57	2543.21	14.8	2523.16	15.4
Feb.	2499.12	2295.20	8.2	2291.24	8.3
Mar.	2585.30	2416.69	6.5	2412.19	6.7
Apr.	1735.20	1429.99	17.6	1395.99	19.5
May	1357.28	1189.04	12.4	1119.24	17.5
June	1333.04	1237.11	7.2	1231.69	7.6
July	733.10	791.11	7.3	799.12	8.3
Aug.	1014.97	922.53	9.1	909.54	10.4
Sep.	2542.29	2172.37	14.6	2121.45	16.6
Oct.	3034.14	2805.23	7.5	2794.99	7.9
Nov.	2882.43	2875.59	0.2	2865.41	0.6
Dec.	3401.58	3487.74	2.5	3499.52	2.8
Average	2175.17	2013.82	9.0	1996.96	10.1

be seen in Table 1 which gives the % error of the predicted available wave power with respect to the actual wave power in 2012. From the comparison, it can be concluded that the wave energy estimates derived using the presented method are available and the accuracy of the approach presented in this study is therefore validated. Table 1 also lists the results given by the EPRI method and demonstrates that the method employed by this paper increases the accuracy of the EPRI method by an average factor of 1.1%.

#### 5 Conclusions

A methodology, which was developed by EPRI based on a modified Gamma spectrum, is presented and revised in this study and employed for analyzing the potential for wave energy conversion in a desired geographic area. This methodology allows WEC developers to easily and effectively predict the potential wave power available to their devices and therefore facilitate the prediction of power output performance in a given year, season, month, etc., in a specific location. The essential part of this methodology is the calibration of the spectral width parameter  $n$  and the spectral peakedness parameter  $\gamma$ . Compared to the original EPRI methodology, the revised method can yield results with a higher accuracy of 1.1% by using Hunt's method to find the wavelength  $L$ . The presented methodology was then applied for the Luke Offshore Test Platform. The case study results showed that such method can deliver robust results in representing the wave climate in a given region where the WECs are deployed and the estimates were close to the data disseminated by National Data Buoy Center. In the future, the methodology presented in this study can be used to map and assess the ocean wave energy resource at any given geographical location in United States.

#### Reference

- [1] "Marine and Hydrokinetic Technology Database," <http://www1.eere.energy.gov/water/hydrokinetic/default.aspx>
- [2] 2007, Preliminary Wave Energy Device Performance Protocol, Department of Trade and Industry, URN 07/808, United Kingdom.
- [3] Smith, G. H., Venugopal, V., and Fasham, J., 2006, "Wave Spectral Bandwidth as a Measure of Available Wave Power," Proceedings of the 25th International Conference on Offshore Mechanics and Arctic Engineering, Hamburg, Germany, June 1–9, Paper No. OMAE2006.
- [4] Saulnier, J.-B., Clement, A., Falcau, A. F. de O., Pontes, T., Prevosto, M., and Ricci, P., 2011, "Wave Groupiness and Spectral Bandwidth as Relevant Parameters for the Performance Assessment of Wave Energy Converters," *Ocean Eng.*, **38**(1), pp. 130–147.
- [5] Kerbiriou, M.-A., Prevosto, M., Maisondieu, C., Clement, A., and Babarit, A., 2007, "Influence of Sea-States Description on Wave Energy Production Assessment," Proceedings of the 7th European Wave and Tidal Energy Conference, Porto, Portugal, Sept. 11–13.
- [6] Kerbiriou, M.-A., Prevosto, M., Maisondieu, C., Babarit, A., and Clement, A., 2007, "Influence of an Improved Sea-States Description on a Wave Energy Converter Production," Proceedings of the 26th International Conference on

- Offshore Mechanics and Arctic Engineering, San Diego, CA, June 10–15, Paper No. OMAE2007.
- [7] Duclos, G., Babarit, A., and Clement, A. H., 2005, “Optimizing of Power Take Off of a Wave Energy Converter With Regard to the Wave Climate,” *ASME J. Offshore Mech. Arct. Eng.*, **128**(1), pp. 56–64.
- [8] Sarmiento, A. J. N. A., Pontes, M. T., and e Melo, A. B., 2003, “The Influence of the Wave Climate on the Design Annual Production of Electricity by OWC Wave Power Plants,” *ASME J. Offshore Mech. Arct. Eng.*, **125**(2), pp. 139–144.
- [9] 2011, Mapping and Assessment of the United States Ocean Wave Energy Resource, EPRI Technical Report No. 1024637, Palo Alto, CA.
- [10] Michael, W. H., 1999, “Sea Spectra Revisited,” *Mar. Technol.*, **36**(4), pp. 211–227.
- [11] Bretschneider, C. L., 1959, “Wave Variability and Wave Spectra for Wind Generated Gravity Waves,” Technical Memo No. 118, Beach Erosion Board, US Army Corps of Engineering, Washington, DC.
- [12] Pierson, W. J., and Moskowitz, L., 1964, “Proposed Spectral Form for Fully Developed Wind Seas Based on the Similarity Theory of S. A. Kitaigorodskii,” *J. Geophys. Res.*, **69**(24), pp. 5181–5190.
- [13] Hasselmann, K., Barnett, T. P., Bouws, E., Carlson, H., Cartwright, D. E., Enke, K., Ewing, J. A., Gienapp, H., Hasselmann, D. E., Kruseman, P., Meerburg, A., Muller, P., Olbers, D. J., Richter, K., Sell, W., and Walden, H., 1973, “Measurements of Wind-Wave Growth and Swell Decay During the Joint North Sea Wave Project (JONSWAP),” *Dtsch. Hydrogr. Z.*, **A12**, pp. 1–95.
- [14] Ochi, M. K., and Hubble, E. N., 1976, “Six-Parameter Wave Spectra,” Proceedings of the 15th Coastal Engineering Conference, Honolulu, HI, July 1–17, pp. 301–328.
- [15] Boukhanovsky, A. V., Lopatoukhin, L. J., and Soares, C. G., 2007, “Spectral Wave Climate of the North Sea,” *Appl. Ocean Res.*, **29**(3), pp. 146–154.
- [16] Boukhanovsky, A. V., and Soares, C. G., 2009, “Modeling of Multi-peaked Directional Wave Spectra,” *Appl. Ocean Res.*, **31**(2), pp. 132–141.
- [17] Soares, C. G., 1984, “Representation of Double-Peaked Sea Wave Spectra,” *Ocean Eng.*, **11**(2), pp. 185–207.
- [18] Torsethaugen, K., 1993, “A Two Peak Wave Spectrum Model,” Proceedings of the 12th International Conference on Offshore Mechanics and Arctic Engineering, Glasgow, Scotland, June 20–24, Paper No. OMAE1993.
- [19] Torsethaugen, K., 2004, “Simplified Double Peak Spectral Model for Ocean Waves,” Proceedings of the 14th International Offshore and Polar Engineering Conference, Toulon, France, May 23–28, pp. 76–84.
- [20] “MMAB Operational Wave Models,” <http://polar.ncep.noaa.gov/waves/#ww3products>
- [21] “Wavewatch III Model,” <http://polar.ncep.noaa.gov/waves/wavewatch/wavewatch.shtml>
- [22] Hsu, S. A., Meindl, E. A., and Gilhousen, D. B., 1994, “Determining the Power-Law Wind-Profile Exponent Under Near-Neutral Stability Conditions at Sea,” *J. Appl. Meteorol.*, **33**(6), pp. 757–765.
- [23] 2004, “Atlas of UK Marine Renewable Energy Resources,” Report No. R1106, Prepared for the UK Department of Trade and Industry, ABP Marine Environmental Research Ltd.
- [24] Hagerman, G., 2001, “Southern New England Wave Energy Resource Potential,” Proceedings of the Building Energy 2001, Tufts University, Boston, MA, March 23.
- [25] 1985, “Direct Methods for Calculating Wavelength,” Coastal Engineering Technical Note No. CETN-1-17, U.S. Army Corps of Engineering, June 4.
- [26] Chen, H.-S., and Thompson, E. F., 1985, “Interactive and Pade’s Solutions for the Water-Wave Dispersion Relation,” Miscellaneous Paper No. CERC-85-4, U.S. Army Engineer Waterways Experiment Station, Vicksburg, MS.
- [27] “National Data Buoy Center, National Oceanic and Atmospheric Administration,” Last Accessed Nov. 18, 2013, [http://www.ndbc.noaa.gov/station\\_page.php?station=42040](http://www.ndbc.noaa.gov/station_page.php?station=42040)